BEZUIDENHOUT, J.J., EKSTEEN, J.J. and BRADSAW, S.M. Computational fluid dynamic modelling of a three-phase electric smelting furnace in the platinum smelting process. *Third International Platinum Conference 'Platinum in Transformation'*, The Southern African Institute of Mining and Metallurgy, 2008.

Computational fluid dynamic modelling of a three-phase electric smelting furnace in the platinum smelting process

J.J. BEZUIDENHOUT, J.J. EKSTEEN and S.M. BRADSAW
Department of Process Engineering, University of Stellenbosch

The electric smelting furnace is commonly used for recovering the valuable PGMs from the bearing ores through the separation of a liquid slag, matte and solid concentrate layer. This multi-phase system plays host to a dynamic interplay between power, temperature and flow, of which a fundamental knowledge would be valuable for maintaining optimum and stable operation.

In an attempt to investigate the furnace system that under practical techniques would be very difficult, Computational Fluid Dynamics (CFD) incorporating electrical potential modelling was applied in a qualitative numerical study for identifying the electrical potential, temperature and flow distributions within the furnace. The commercial CFD package Fluent 6.3.26 (2006) was used to model an 11 m diameter circular, three-phase electrical furnace.

A full-scale, three-dimensional model furnace from the bottom to the top concentrate layer was created. The fluid-fluid interaction between the slag and matte layer was facilitated through the application of the volume of fluid (VOF) multi-phase model while a three-phase AC current was applied at a reduced frequency to electrodes resembled by volume sources. Energy-sinks were user-defined to account for the melting of concentrate as well as the heat-up of material due to the absence of in- and outflow boundaries.

The model outcome presents an electric potential distribution very close to previous studies and within the actual furnace operating range. The current was found to flow via the more conductive matte layer between the electrodes, resulting in the majority of the resistive heat generation to be concentrated within the immediate slag surrounding the electrodes. The temperature profiles indicated the slag to be at a uniform temperature due to effective mixing resulting from buoyancy forces. The temperature distribution within the concentrate and matte layers were found to be stratified.

Introduction

The electric smelting furnace is used within platinum smelting process for concentrating the valuable metals in a Ni-Cu-Fe-S matte prior to refining. The electric smelting furnace is best described as a complex system. The extensive heat generated through resistive heating promotes the separation of a gangue-rich slag layer and a precious metal-rich matte layer based on the principle of density difference. The furnace therefore hosts a multidimensional, multi-phase system where flow is induced by gas bubbles from the electrode tips, buoyancy and slight magnetic influence. Each material layer contained within the furnace walls possesses a character expressed by a unique set of non-linear properties that describe its interaction with the heat and current gradients brought forth by the electrodes.

This dynamic system is susceptible to a vast number of influences of which the material layer depth, feed composition, and electrode immersions are the main control parameters that are continuously adjusted by a sophisticated control system to maintain optimum operation. It is evident that a comprehensive knowledge of the furnace behaviour is required to expand and improve the current operation and throughput. The extreme process conditions do not, however, permit uncomplicated evaluation of the furnace interior and one is left with only external parameters to mirror the behaviour on the inside.

Commercial Computational Fluid Dynamics (CFD) has been initially developed for mechanical applications but has fairly recently found its way to the modelling of processes in the metallurgical engineering industry. CFD can be viewed as a powerful engineering toolkit for creating virtual computer prototypes of processes that would under the actual operating conditions be impossible to predict and quantify. A CFD model that would resemble the electric smelting furnace as closely as possible is therefore regarded as an invaluable asset for describing the interior dynamics that could lead to potential optimization of the present unit.

Previous CFD models on the electric furnace of various complexities have been attempted but still fall short of providing a complete and accurate model representation. Several phenomena such as multiphase layers, gas dispersion, smelting of material and a dynamic AC electrical power supply are yet to be addressed. In the present study, advantage is taken of the most recent advances in commercial CFD software to further the modelling of the circular three-phase electric smelting furnace towards an ideal holistic representation.

The electric furnace in the platinum smelting process

The electric furnace finds itself at the heart of the platinum recovery process and is the primary unit for separating the

gangue from the valuable constituents. Prepared concentrate is fed through the furnace roof to form the upper concentrate layer that inherently shields the furnace roof and freeboard from the most of the potential heat loss through radiation, and therefore retaining heat in the melt. The concentrate layer settles to become molten within the underlying slag layer while matte droplets, being denser, diffuse through the slag layer and settle on the furnace hearth to form the matte layer. The slag layer therefore consists mostly of molten oxides and silicates while the matte layer retains the valuable metal sulphides.

However, due to the recent smelting of high chromium-bearing concentrates, intermediate layers of chromium spinel are likely to form. These deposits have been known to make the operability of the electric furnace very difficult, especially for preventing effective slag-matte separation. To compensate, the electric furnace is operated at higher temperatures with the hope of increasing the Cr_2O_3 solubility. Magnitite (Fe_3O_4) precipitations are also likely to form at the slag-matte interface that is believed to be increased by turbulence within the slag layer[1]. Knowledge of the temperature and flow distributions within the furnace would therefore be advantageous for predicting regions where these deposits are likely to occur.

The three-phase AC current is supplied to the molten bath through three carbon electrodes that are arranged in a delta formation. Within this electric smelting circuit, the electrical resistances of the electrodes and the furnace refractory are negligible compared to the resistance posed by the furnace charge and slag layer. The electric resistance of the matte layer is also significantly lower than the slag layer, therefore making the slag layer the mayor source of heat generation (also called Joule heating) within the furnace. Previous studies performed on the electric furnace have shown the majority of the electrical current, finding the path of least resistance, to pass via the matte layer between the electrodes[2].

The reduction at the carbon electrodes is likely to form CO gas bubbles that in turn create a gas layer covering the immersed electrode tip. A consequent localized voltage drop is expected due to the formation of small electrical arcs from the electrode tip as breakdown potential of the gas is reached and electrical current is allowed to pass through the gas layer. This voltage drop has been estimated at 35-40% of the applied furnace potential for sufficient electrode immersion[3]. A previous CFD study by Sheng *et al*.[4] investigated and incorporated the phenomenon of a localized voltage drop at the immersed electrode surface and reported a voltage drop of 100–120 V for applied potentials of 180–230 V[4]. This character of the electric smelting furnace was kept in mind during the development of the CFD model.

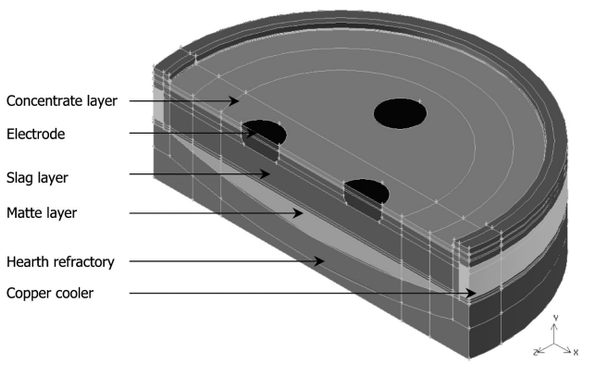

Figure 1. The furnace geometry and material layers

Model development

Geometry

A review of previous modelling attempts on the circular furnace revealed a general simplification in the modelling by means of symmetrical division of the computational domain. These attempts, however, do not include a time-variant power input that is likely to lead to asymmetrical behaviour, especially in electrical field and current density due to the varying current paths between the electrodes. An investigation into the dynamics and influences on the slag and matte layers will therefore require the modelling of the full, three-dimensional furnace geometry and the inclusion of the electrodes for establishing three-phase energy input.

This required a model of considerable computational capacity. It was therefore considered a sound approximation to model only the bottom part of the furnace up to the concentrate layer, neglecting the furnace freeboard and roof. The three-dimensional, 11 m diameter furnace geometry was created in the preprocessing package Gambit 2.3.16 (2006) and was based on the actual furnace dimensions. The specific material layers were assigned to the geometry, as depicted in Figure 1. The electrodes were initially modelled as cylindrical volumes but were later rounded along the bottom edges to represent the phenomenon of 'pencilling' as commonly found during actual operation. The geometry that was created incorporated a 35% electrode-slag immersion.

Physical properties

The physical properties, tabulated below, were obtained from various literature sources and assigned to the material layers. The density and viscosity of the material layers were specified as piecewise linear functions so as to incorporate variability due to temperature difference while general refractory properties were assigned to the furnace hearth and walls. As stated, the high resistivity of the slag layer is the controlling variable for heat generation within the furnace. The electrical conductivity of the slag was

Table I
Physical properties

Physical properties of the slag layer	
Density (kg/m^3)	2 775.74 – 2 474.06
Viscosity (kg/m.s)	0.123
Specific heat (J/kg.K)	1373
Thermal conductivity (W/m.K)	2.3
Electrical conductivity (mho/m)	34
Physical properties of the matte layer	
Density (kg/m^3)	4 428.99 – 3 871.60
Viscosity (kg/m.s)	0.0032
Specific heat (J/kg.K)	890
Thermal conductivity (W/m.K)	17
Electrical conductivity (mho/m)	9 3000
Physical properties of the concentrate layer	
Density (kg/m^3)	1 400
Specific heat (J/kg.K)	1 100
Thermal conductivity (W/m.K)	1.2
Electrical conductivity (mho/m)	1.2

therefore continuously adjusted so as to maintain a constant heat input according to the energy-balance that was performed beforehand. The chosen electrical conductivity was however well within the range associated with PGM-bearing concentrates[6].

Computational grid

An appropriate computational grid was fitted to the created geometry in Gambit 2.3.16. The mesh consisted of good quality hexahedral elements with the worst element having a skewness ratio of 0.456. A grid-independent study was performed during the initial simulations and the immediate area surrounding the electrode was identified to contain high gradients of current density and electric potential. The grid was therefore refined in a cylindrical area surrounding the electrodes, bringing the total cell count to 643 090 hexahedral elements.

Boundary conditions

The model boundary conditions were specified to resemble the actual furnace as closely as possible. This included a thermal-boundary at the top of the concentrate layer with a constant heat transfer coefficient of 25 W/m.K and a free-stream temperature of 833 K. The sidewalls and hearth of the furnace-model were assigned a heat transfer coefficient of 100 W/m.K and a free-stream temperature of 27°C. These convection boundary conditions were assigned based on the furnace energy balance for maintaining a balanced energy output. The inner furnace walls as well as the outer surface of the electrodes in contact with fluid were specified as non-slip wall boundaries. Electrical boundary conditions were specified for the outer furnace walls at ground potential and the top surface of the electrode volumes were specified as conducting walls with a zero current density to permit the in- and outflow of electrical current.

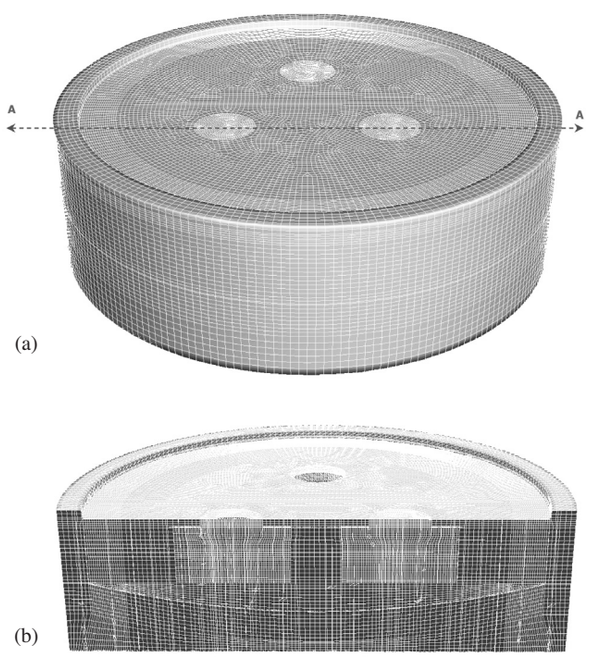

Figure 2. (a) The computational grid fitted to the furnace geometry (b) a cross-sectional view AA, showing the refinement in a cylindrical area around the electrodes

Model specifications

The commercial CFD package Fluent 6.3.26 (2006) was used for the CFD calculations. To couple the modelling of electrodynamics, the magneto-hydrodynamic supplement MHD 2.1 (2006) allowed the specification of an electrical current input and the calculation of resistive heat. The time-dependent three-phase AC current required the model equations, generalized by Equation [1], to be solved in a transient manner by using a pressure-based solver[7].

$$\nabla \cdot \left(\rho \vec{V} \phi \right) = \nabla \cdot \left(\Gamma^{\phi} \text{grad}\, \phi \right) + S^{\phi} \qquad [1]$$

For this equation:

- ϕ : The dependent flow variable representing the velocity component, temperature, turbulence kinetic energy or its dissipation rate, etc.
- $\vec{V}$: Velocity vector
- ρ : Density of the fluid phase
- $\Gamma\phi$: Diffusion coefficient
- $S\phi$: General source term relevant to the variable ϕ[7]

Electrodynamic specifications

The electric potential method was selected within the magneto-hydrodynamic solver to couple the electrodynamic modelling with the CFD modelling and for specifying current density power inputs. This method incorporates Maxwell's equations of electrodynamics for determining the electrical potential throughout the domain. The electric potential method does not, however, include the influence of an induced magnetic field, brought about through the flow of current according to Ampere's law. An evaluation of the magnetic Reynold's number proved the convection of a magnetic field and magnetic boundary layers to occur within the high current density areas to be unlikely. Flow within the bath was further estimated to be buoyancy-driven through a quantitative comparison between the magnitude of the velocity induced through natural convection and Lorentz-driven flow, performed according to the method presented in Davidson[8]. Choudhary and Szekely[9] proved this finding experimentally and were adapted in the previous modelling study by Sheng[5]. To further substantiate this simplification, it is known that the molten concentrate is well above the Curie temperature, a temperature above which all ferro-magnetic material become paramagnetic[10]. It is therefore expected that an induced magnetic field would have very little effect on the flow and temperature distribution within the furnace; however full magneto-hydrodynamic effects still need to be investigated to acquire full confidence in the model.

The resistive heat (q) generated within the material layers is included within the energy equation by means of the following source term:

$$q = \frac{J^2}{\sigma} \qquad [2]$$

For the Equation [2], J is the current density (A/m^2) and σ the electrical conductivity (mho/m).

Multi-phase specifications

It was stated that the electric furnace hosts a multi-phase system of different material layers. Due to the computational difficulty, no interface layer of chromium spinel was assumed and only the slag layer with the

underlying matte layer was modelled as multi-phase fluid layers. In order to model two contacting fluids, the volume of fluid (VOF) multi-phase model was incorporated in the modelling approach. The VOF model allocates continuity equations for each phase and keeps track of the interpenetrating continua through a fluid fraction function that represents the volume fraction of a computational cell that is occupied by the specific fluid[11]. For the current model, the slag phase was selected as the primary and matte as the secondary phase.

To establish an interface between the two fluids, the CICSAM (comprehensive interface capturing scheme for arbitrary meshes) interpolation technique was selected as being specifically suitable for modelling the interface between fluids with big differences in viscosity and providing a much required numerical stability[11]. An interfacial tension of 0.4 N/m was specified to be acting between the slag and matte layer[12].

Power input

To facilitate the modelling of a three-phase alternating current, energy sources were allocated to the volumes representing the electrodes. These current sources were specified as sinusoidal functions, equall in magnitude but lagging by 120°, through user-defined functions (UDFs) written in C++. An important assumption had to be made regarding the current frequency. The actual current frequency of 50 Hz would require an extremely small time-advancement in the transient solving of the model equations. For this reason, a current input with a frequency of 0.0167 Hz (1 minute period) was specified. The extent of this assumption was investigated through its effect on the temperature and flow distributions within the melt. Slight temperature peaks of 1% of the maximum temperature and 0.6% in the average matte velocity were observed, which under the actual frequency would not be present. These small variations are regarded as negligible and the reduction in frequency was therefore regarded as an adequate assumption.

Material heat-up and heat of melting

In the actual furnace, the slag and matte layers are tapped regularly, therefore causing the material within the furnace to descend as fresh concentrate is introduced at the top. A considerable amount of energy is therefore associated with the heat-up of the material between the in- and outflow of the furnace. To reduce the computational expense of modelling a moving multi-phase system, energy sinks were created to imitate the heat-up of the descending material. The change in enthalpy (H) was achieved by a user-defined function based on Equation [3].

$$\Delta H = \dot{m}.c_p.(T_{cell} - T_{ref}) \quad [3]$$

For this equation, m is the mass flow-rate (kg/s), which was taken as the concentrate feed-rate to the furnace, c_p the specific heat capacity (J/kg.K) and T the temperature (K) of either the computational cell or the reference temperature. The reference temperatures for the concentrate layer and slag layer were taken as the surface temperature and melting temperature, 1 523 K, respectively.

The heat of melting was estimated by performing a set of thermodynamic simulations for the typical processed ore within the temperature range 800 to 1 800°C. This was performed with the aid of the commercial thermodynamic solver FactSage®[13]. As an example, Figure 3 indicates the initialization of melting at 1 200°C—clearly seen by the steady increase in enthalpy. The normal enthalpy gradient is resumed at 1 400°C. The resulting change in enthalpy was calculated at 4.28 MW for the respective concentrate feed-rate.

The allocation of this amount of smelting energy was performed by identifying distinctive smelting zones within the concentrate layer according to the likelihood of smelting occurring within a particular zone. The interface between the slag and concentrate layer were identified as a high concentration point for smelting. A very thin 50 mm layer was created at the interface and further subdivided into three different radial zones to imitate the radially decreasing rate of melting. To maintain a steady energy distribution, 30% of the calculated heat of melting was allocated to the thin interfacial layer, and the remaining 70% were assigned to the upper part of the concentrate layer, above the 50 mm layer. To enable a logical distribution of temperature through the concentrate layer, it was decided to allocate the melting energy for the 50 mm layer in the ratio of 60:25:15%, as depicted in the inset of Figure 3 to represent radial smelting as closely as possible.

Solving

The Pressure-Implicit with Splitting of Operators (PISO) scheme was selected within the Fluent solver to allow pressure-velocity coupling due to its ability for enhancing numerical stability and being particularly suitable for simulating transient flows. In order to obtain a stable numerical solution, a conservatively small transient time-step was used for the initial iterations. After steady residuals were established, the time-step size was increased to 0.05 seconds which is an adequate time-period for capturing the character of the 1-minute period sinusoidal current inputs.

A parallel processing system was established due to the large computational requirement of the furnace model. The parallel system consisted of four dual core computers, three of which had 3.3 GHz processors and one having 1.8 GHz processors. For this reason, twice as many cells were allocated to the more powerful nodes. To effectively divide

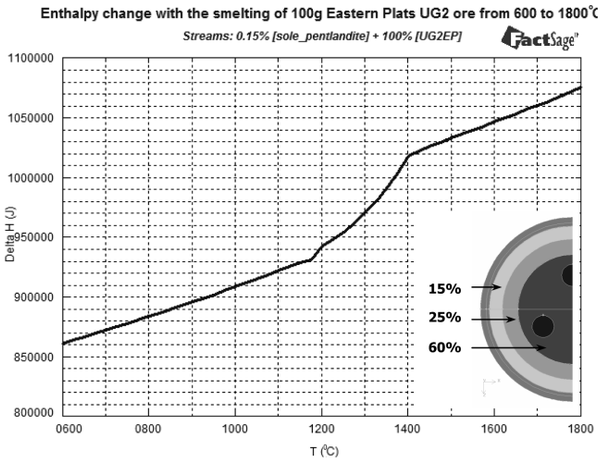

Figure 3. An example of a thermodynamic simulation for determining the heat associated with melting. Also shown is the allocation of the heat of melting within the concentrate layer.

the amount of cells for parallel processing, the Metis partitioning method was selected due to its ability for minimizing the number of partition interfaces and the number of partition neighbours[11]. A transient time of approximately two hours were simulated to obtain a steady state condition for the model variables.

Simulation results

Electric potential

The electric potential distribution within the concentrate, slag and matte layers is presented in Figure 4. The three-phase current input is clearly depicted, showing the two electrodes on the right-hand-side to be at a current input stage and the electrode furthest to the left to be receiving current.

The voltage at the electrode surface compares very well to the measured electrode potential at the surface. A sharp radial decrease in the electric potential (shown in Figure 5) is observed from the electrode surface towards the outer furnace walls. This also compares very well to the previous studies by Sheng *et al*.[5] and Xia *et al*.[14] The difference between the actual overall voltage measured on the furnace and the calculated voltage at the surface is attributed to the occurrence of arcing at the electrode surface that results in considerable power dissipation.

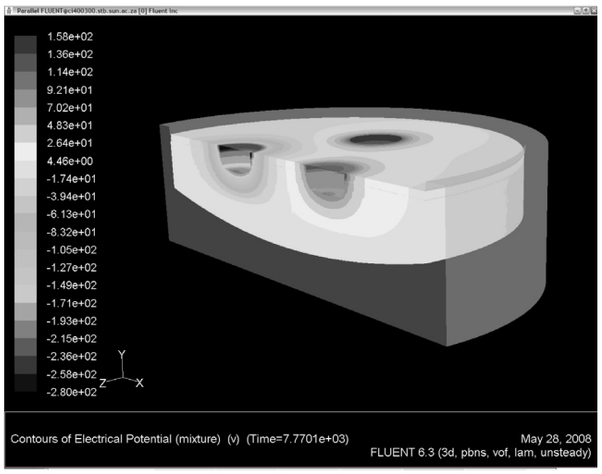

Figure 4. Electric potential (*V*) distribution within the concentrate slag end matte layers

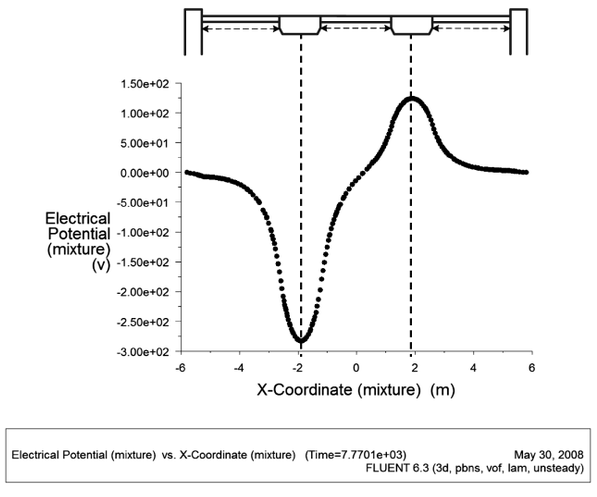

Figure 5. Electric potential (*V*) distribution measured along a horizontal line though the front two electrodes of the furnace

Current density

The current density distribution is in good accord with the electrical potential distribution. A spherical current distribution is observed around the electrode tips that fade rapidly towards the furnace side. This compares well with the findings of Utigard *et al*.[2] From the electrodes, the current is seen to make its way towards the matte layer where it flows towards the receiving electrode (the detail vector plot is provided in Figure 7). Very little current passes between the electrodes through the slag layer. This is in good agreement with the discussion by Barth[1], stated previously, that reports the majority of the current to pass

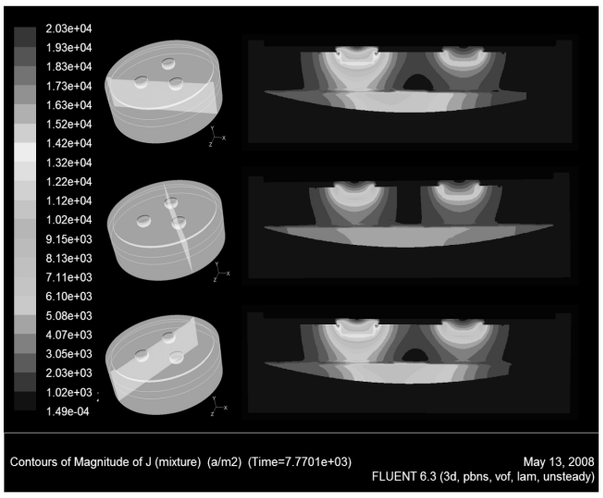

Figure 6. Current density distribution at various vertical sections through the electrodes

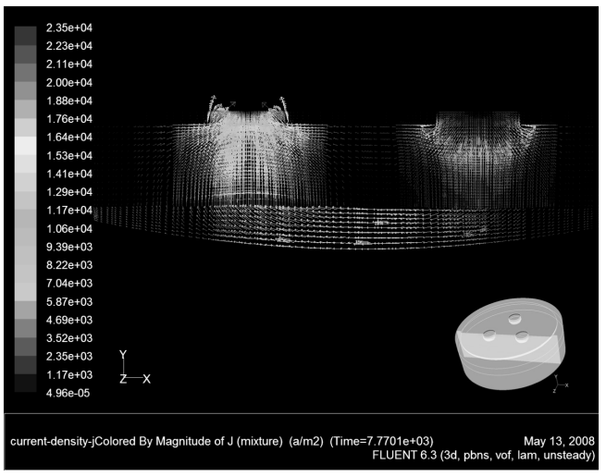

Figure 7. Current density vectors on a vertical plane through the front two electrodes, showing the current flowing from the right electrode down towards the matte layer and up towards the left receiving electrode

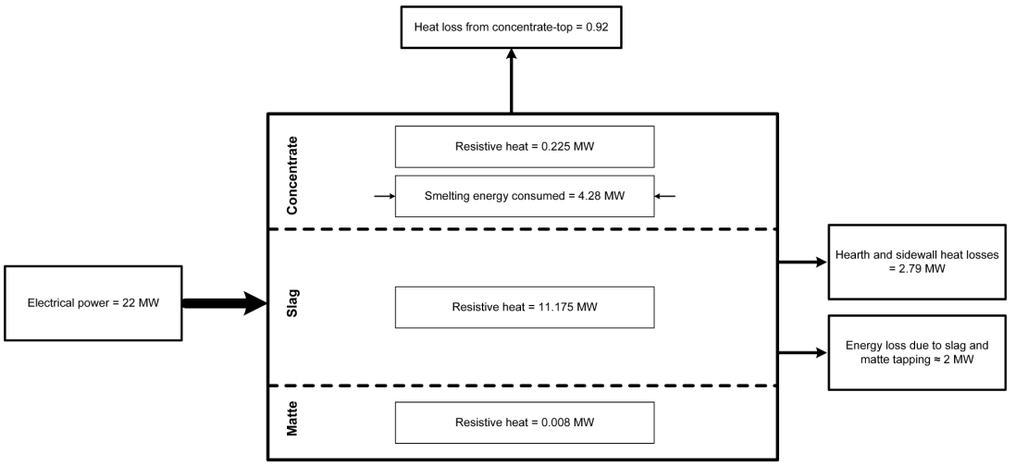

Figure 8. Furnace energy balance

via the matte layer between electrodes due to the considerable high electrical conductivity of the matte layer.

Furnace power and energy balance

The present model incorporated a current input of 40 kA, relating to a furnace electrical power input of 22 MW. As discussed, the slag electrical conductivity was adjusted throughout the simulation to retain the required amount of energy within the furnace according to the energy-balance. A schematic of the energy balance is provided in Figure 8. The difference between the furnace electrical power input and overall energy losses amount to an energy accumulation of 12.01 MW within the furnace. The total amount of resistive/Joule heat calculated from the furnace model amounts to 11.41 MW of which 97.96% is attributed to the slag. The difference between the in- and outflow of energy and the amount accumulated through resistive heat is considered the result of further energy losses that were not taken into account. The energy loss due to arcing is considered the most defining energy loss neglected.

Velocity distribution

Motion within the melt is induced through buoyancy forces that are made possible through the specification of a temperature-dependent density property for the material layers. The resulting velocity profiles show the molten bath to be well mixed and asymmetrical. The highest flow is observed around the electrode at which the highest power is concentrated. The horizontal contour plot, Figure 10, shows the flow to be asymmetrical and three-dimensional with the highest flow regions between the electrodes and near the sidewalls. Very little flow is observed within the matte layer, except at the slag-matte interface. The velocity at the interface is presumed to result from a drag-force exerted by

Table II
Velocities within the fluid layers

Material layer	Average velocity (m/s)	Maximum velocity (m/s)
Slag	0.0058	0.0363
Matte	0.0043	0.0218

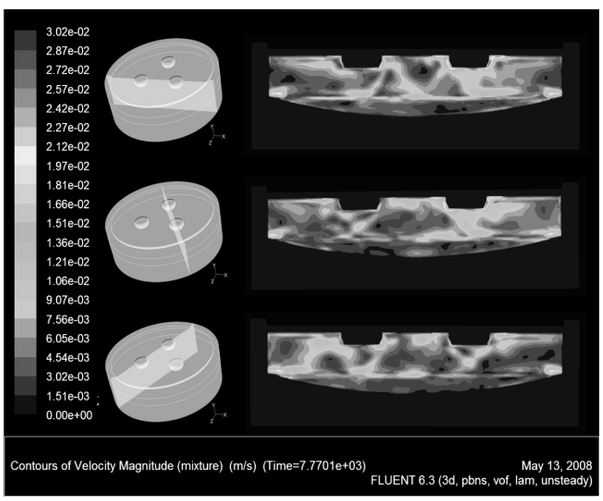

Figure 9. Velocity contours along various vertical sections through the electrodes

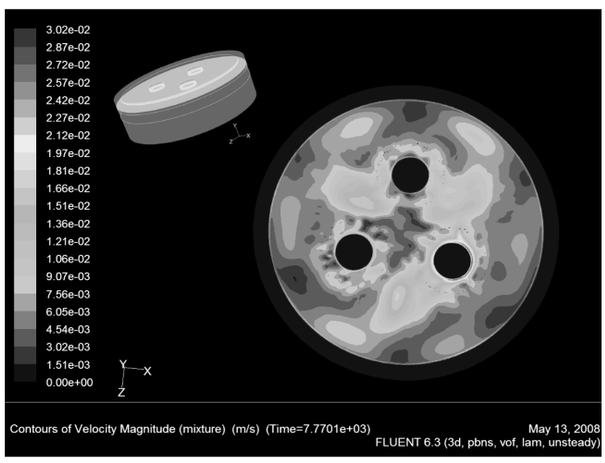

Figure 10. Velocity contours along a horizontal section through the upper part of the furnace and through the electrodes

Table III
Temperatures within the material layers

Material layer	Average temperature (K)	Maximum temperature (K)
Slag	1 917	1 991
Matte	1 692	1 866
Concentrate	1 524	1 976

the slag layer, having the higher viscosity. Figure 11 shows the slag rising underneath the electrode where it is heated and moving to the furnace sidewall where it cools and descends.

The flow profiles that were obtained are simulated under laminar flow conditions since the incorporation of a turbulence model resulted in the model becoming unstable. The assumption of laminar flow is however justified by the very low velocities observed within the slag and matte layer and it is expected that turbulent fluctuations will be damped out by the slight electromagnetic forces experienced by the molten bath[15].

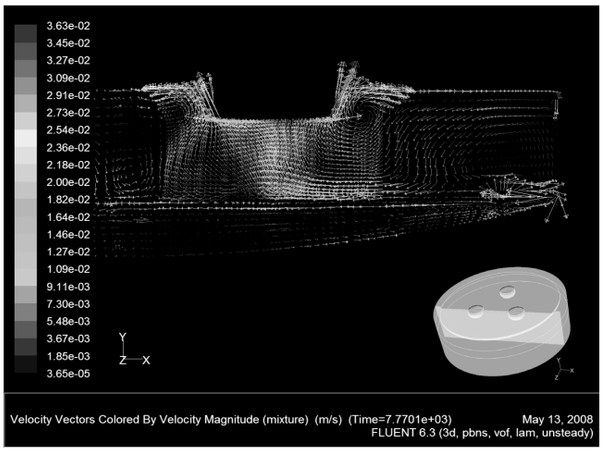

Figure 11. Velocity vectors on a vertical plane through the front two electrodes

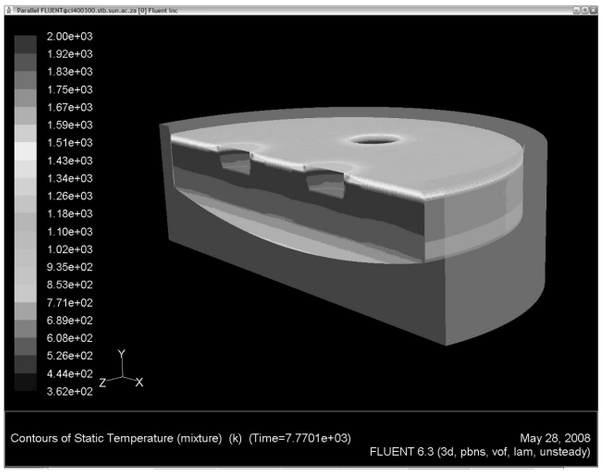

Figure 12. Temperature contours of the concentrate, slag and matte layers

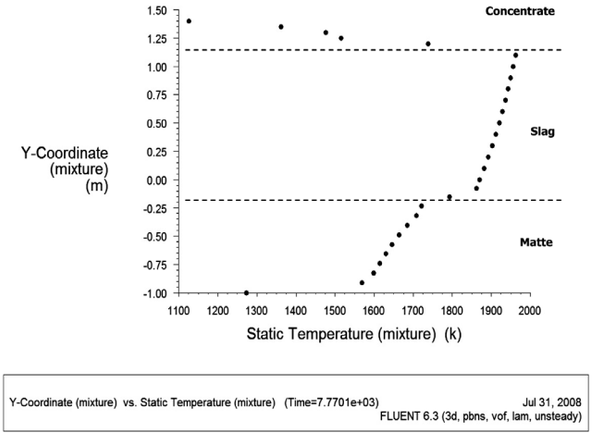

Figure 13. Temperature measurements taken at various points along a vertical line running through the centre line ($x = 0, z = 0$) of the furnace

The average and maximum velocities for the slag and matte layer are close in magnitude. Carbon monoxide bubbles, forming at the immersed electrode surface and dispersing through the upper slag towards the concentrate layer, are expected to increase the maximum velocity within the slag layer and contribute to mixing, but due to the high computational requirement it has not been modelled.

Temperature distribution

The calculated average temperatures for the slag and matte layers compare closely to the actual tapping temperatures. The temperature within the slag layer was found to be fairly uniform, while a stratified temperature distribution is observed in the concentrate and matte layers.

A vertical temperature profile, presented in Figure 13, compares very well to the temperature distribution presented in the study by Sheng *et al.*[5] A very sharp drop in temperature is seen within the concentrate layer. The average temperature within the concentrate layer is lower than the concentrate melting temperature, indicating the presence of a solid layer as is the case with the actual operation of the furnace.

Future work

Because of the difficulty of maintaining a numerically stable solution, the effect of turbulence on the flow profile has been omitted. An attempt will be made to include turbulence along with additional momentum sources resulting from CO gas bubble formation at the immersed electrode tips.

Conclusions

A full-scale, three-dimensional CFD model has been created for the three-phase current, circular electric smelting furnace. The advances in CFD were applied along with electric potential modelling to obtain the power, flow and temperature distributions characteristic of the furnace. The model also incorporated both the slag and matte layers as fluid continue through the use of the VOF multi-phase model. The actual three-phase AC current was approximated by a 0.0167 Hz sinusoidal current supply to volume sources representing the electrodes. Further user-

defined functions were used to include the heat consumption due to melting, calculated at 4.28 MW, within the concentrate layer and the heat-up of the material as it descends, which in the actual operation will represent the in- and outflow of material.

The electrode potential distribution compares well with the actual operation while also showing a distinctive radial drop. This distribution is complemented by the current through the bath, where the majority of the current was found to flow via the matte layer between the electrodes. Following this rapid radial decrease in electrical current around the electrode, the resistive heat was found to be concentrated in the immediate slag surrounding the immersed electrode surface.

The slag layer was observed to be well mixed by complex, asymmetrical flow driven by natural buoyancy forces. Very little flow was present within the matte layer where the maximum flow was observed near the slag-matte interface. As a result of the well-mixed slag, the temperature distribution was found to be uniform. The temperature profiles within the concentrate and matte layers were stratified.

Confidence in the model results is confirmed through good comparison to the actual operation of the electric furnace and close agreement to previous modelling studies.

Acknowledgements

The authors would like to thank Stephan Schmitt and Danie de Kock from Qfinsoft, the agents for Fluent® in South Africa, for their technical support. The sponsorship from the National Research Foundation is kindly acknowledged.

References

1. BARTH, O. Electric smelting of sulphide ores, extractive metallurgy of copper, nickel and cobalt, Queneau, P. (ed.), Metallurgical Society of AIME, 1960. pp. 241–262.
2. UTIGARD, T., RENNIE, M.S. and RABEY, C.C. The smelting of copper-nickel concentrates in an electric furnace, Proceedings of the International Symposium on Copper Extraction and Refining, Las Vegas, Biswas, A.K. and Davenport, W.G. (eds.), TMS-AIME, Warrandale, PA, February 1976. pp. 22–26.
3. TSEIDLER, A.A. Metallurgy of Copper and Nickel, Ministry of Education of the U.S.S.R., 1958, Translated from Russian by Israel Program for Scientific Translations. 1964.
4. SHENG, Y.Y., IRONS, G.A. and TISDALE, D.G. Transport phenomena in electric smelting of Nickel matte: Part I – Electric potential distribution, *Metallurgical and materials transactions B*, vol. 29B, 1998. pp. 77–83.
5. SHENG, Y.Y., IRONS, G.A. and TISDALE, D.G. Transport phenomena in electric smelting of Nickel matte: Part II – Mathematical modelling, *Metallurgical and materials transactions B*, vol. 29B, 1998. pp. 85–94.
6. HUNDERMARK, R. The Electrical conductivity of melter type slags, MScEng thesis, University of Cape Town, June. 2003.
7. PATANKAR, S.V. Numerical heat transfer and fluid flow, Hemisphere, 1980. pp. 11–17.
8. DAVIDSON, P.A. *An introduction to magnetohydro dynamics*, Cambridge University Press, 2001. pp. 3–40 and 324–347.
9. CHOUDHARY, M. and SZEKELY, J. Some general characteristics of heat and fluid flow phenomena in electric melting and smelting operations, *Transactions of the Institute of Mining and Metallurgy*, Section C, vol. 90, 1981. pp. 164–173.
10. AHARONI A. *Introduction to the theory of ferro magnetism*, Oxford Clarendon. 1996.
11. FLUENT 6.3, 'User's Guide', September 2006.
12. SUNDSTRÖM, A.W., EKSTEEN, J.J. and GEORGALLI, G.A. Review of viscosity, density, surface-and interfacial tension of base metal mattes, submitted to: *Journal of South African Mining and Metallurgy*. 2008.
13. BALE, C.W., CHARTRAND, P., DEGTEROV, S.A., ERIKSSON, G., HACK, K., BEN MAHFOUD, R. MELANÇON, J., PELTON, A.D., and PETERSEN, S. FactSage thermochemical software and databases, *Calphad Journal*, vol. 26, ed. 2, 2002. pp. 189–228.
14. XIA, J.L and AHOKAINEN, T. Numerical modelling of slag flows in an electric furnace, *Scandinavian Journal of Metallurgy*, vol. 33, 2004. pp. 220–228.
15. SZEKELY, J. *Fluid flow phenomena in metals processing*, Academic Press, 1979. pp. 175–183.

Johan Bezuidenhout
Masters Student, University of Stellenbosch

Johan Bezuidenhout obtained his degree in Chemical Engineering from the University of Stellenbosch un 2006. He is currently studying towards his Masters degree in Metallurgical Engineering at the University of Stellenbosch